Colloids and Surfaces B: Biointerfaces 114 (2014) 11–19

Contents lists available at ScienceDirect

Colloids and Surfaces B: Biointerfaces

journal homepage: www.elsevier.com/locate/colsurfb

Synthesis and characterization of biocatalytic γ-Fe_2O_3@SiO_2 particles as recoverable bioreactors

A.M. Vaz, D. Serrano-Ruiz, M. Laurenti, P. Alonso-Cristobal, E. Lopez-Cabarcos, J. Rubio-Retama*

Department of Physical-Chemistry II, Faculty of Pharmacy, Complutense University of Madrid, 28040 Madrid, Spain

ARTICLE INFO

Article history:
Received 16 April 2013
Received in revised form
23 September 2013
Accepted 26 September 2013
Available online 8 October 2013

Keywords:
Enzymes
Magnetic nanoparticles
Bioreactors

ABSTRACT

In this work, we present a suitable methodology to produce magnetically recoverable bioreactors based on enzymes, which are covalently attached on the surface of iron oxide@silica nanoparticles. In order to produce this system, iron oxide clusters with a mean diameter of 68 nm were covered with silica. This strategy yields spherical γ-Fe_2O_3@SiO_2 cluster@shell nanoparticles with a mean diameter of 200 nm which present magnetic responsiveness and enhanced stability. The surface of these nanoparticles was modified into two steps with the aim to obtain carboxylic functional groups, which were activated to react with the enzyme glucose oxidase (GOx) that was thus immobilized on the surface of the nanoparticles. The objective of this chemistry at the nanoparticles interface is to produce magnetic-responsive bioreactors. The enzymatic activity was evaluated by using the recoverable bioreactors as part of an amperometric biosensor. These measurements allowed determining the stability, catalytic activity and the amount of enzyme immobilized on the surface of the nanoparticles. Furthermore, the functionalized nanoparticles can be recovered by applying an external magnetic field, which allows them to be employed in chemical processes where the recovery of the biocatalyst is important.

1. Introduction

In recent years, different technological fields like molecular-biology or pharmaceutical chemistry have focused on the production of complex organic molecules, whose synthesis requires the use of biocatalysts such as enzymes. Most of these biomolecules are expensive, and their reuse has prompted scientists to develop a variety of processes that allow to fix them on solid support with the aim of recovering and/or re-utilizing them [1,2]. Some of these processes are based on enzyme entrapment within a polymer matrix, yielding a catalytic system with high enzymatic stability. In this methodology, the polymer network wraps the biological components avoiding its denaturalization during the catalytic reaction [3].

However, these systems are not appropriated when products or substrates with high molecular weight are involved in the reactions, since the diffusion of these molecules is hampered by the polymer matrix. To overcome this problem, a dazzling variety of strategies have been developed. Some authors immobilize the biological component on the surface of different supports such as mesoporous silica [4], molecular sieve [5], membranes [6], epoxy polymers [7], anion exchange resins [8]. Thereby, the access of the substrates and the release of the products are not hindered, favoring reactions in which high molecular weight substrates or products are involved. To enhance the catalytic activity of these systems, nanoscale materials have focused a great interest because of their very large surface to volume ratio in comparison with traditional macroscale materials [9–11], permitting the immobilization of higher amount of biological components. Among other nanomaterials, magnetic nanoparticles have gained a growing interest as immobilization support, since they are easily synthesized, present a very large specific surface and magnetic responsiveness that facilitate their separation [25,27,30]. In spite of these characteristics, their poor colloidal stability at neutral pH makes necessary its functionalization [12]. For this reason, surface modification has become a fundamental step to provide colloidal stability as well as anchoring points where biological components can be immobilized. Among others, the use of polymer shells covering the magnetic nanoparticles is one of the most used strategies [26,28,29]. In this strategy, the polymer shell constitutes an interesting platform where the biological components can be attached by exploiting electrostatic or covalent interactions. Another interesting strategy consists on coating the magnetic nanoparticles with amorphous silica, which should improve significantly the colloidal stability of the resulting material [13,14]. In addition, silica chemistry is easy, inexpensive, and allows to immobilize any kind of molecule in few steps.

* Corresponding author. Tel.: +34 913941751; fax: +34 913942032.
E-mail address: bjrubio@ucm.es (J. Rubio-Retama).

0927-7765/$ – see front matter © 2013 Elsevier B.V. All rights reserved.
http://dx.doi.org/10.1016/j.colsurfb.2013.09.051

The silica coating of inorganic nanoparticles can be carried out using two different strategies. One is based on a reverse-microemulsion method [15], which produces core–shell silica particles pretty much monodisperse, with a controllable shell thickness and a core constituted by a single inorganic nanoparticle. In spite of these advantages, this method might require much effort to separate the core–shell nanoparticles from the large amount of surfactant associated with the micro-emulsion [16]. A surfactant-free alternative is based on the well-known Stöber process [17]. Here, the silica is formed "in situ" through the hydrolysis and condensation of a sol–gel precursor [18,19]. This process can produce core–shell particles by using nanoparticles as seeds for the silica deposition, But, for this to happen, it is necessary to have inorganic nanoparticles stable in the alcoholic reaction medium. This fact has prompted scientists to use for instance capping agents such as (3-aminopropyl)trimethoxylsilane, which stabilizes and promotes the silica growing during the reaction [20]. Other authors employed polymers like poly(vinylpyrrolidone) (PVP) to cover the surface of the nanoparticles with the aim of increasing their stability. Although this method is straightforward, the selection of the polymer strongly influences the homogeneity and smoothness of the silica shell [21].

An alternative to these methods is presented in this work. Our strategy is based on the formation of hydrophobic nanoparticles that are stabilized with a non-ionic surfactant. In this way, stable colloidal magnetic clusters are obtained, which can act as seeds for the silica deposition. The results of these reactions were magnetic silica hybrid nanoparticles with a mean diameter of 200 nm. The surface of these particles was subsequently modified to attach covalently enzymes, creating in this way recyclable bioreactors.

The methodology presented in this work differs significantly from the recently published by Stanciu et al. [31] which exploited the electrostatic interactions for coupling the silica particles and the enzymes. Although the method proposed by Stanciu is simple in terms of preparation, the weak interactions established between the enzyme and the particles could affect the enzymatic activity and stability, decreasing the reusability of the material. In this work we discuss the benefit that would suppose the covalent immobilization of enzymes on the loading capacity, catalytic activity and stability of the bioreactors.

2. Experimental

2.1. Materials

Estearic acid, iron (III) chloride, iron (II) chloride tetrahydrate, succinic anhydride, (3-aminopropyl), amino propyl triethoxysilane, toluene, 6-[fluorescein-5(6)-carboxamido]hexanoic acid N-hydroxysuccinimide ester and glucose oxidase were purchased from Sigma. Polyoxyethylenesorbitan(80) monooleate (P80), tetraethyl orthosilicate (TEOS), N-ethyl-N8-dimethylaminopropyl-carbodiimide (EDC), N-hydroxysuccinimide (NHS) were purchased from Fluka. Ammonium hydroxide, ethanol, hexane and chloroform were purchased from Panreac.

2.2. Characterization

The particles were studied using transmission electron microscopy (TEM) JEOL 1010 and JEOL 2100, working at 80 kV and 200 kV, respectively. The FTIR spectra were taken with a Nicolet IR200 FTIR. The DLS measurements were recorded using a Zetasizer Nano ZS (Malvern Instruments). The correlation function was used to calculate the *Z*-average (intensity mean) and hydrodynamic diameter (D_h) using the Einstein–Stokes equation. This evaluation was performed by selecting the multimodal analysis method of the DTS software (5.0) provided by Malvern. Magnetization was measured using a SQUID class MPMS from Quantum Design working at 25 °C and scanning magnetic fields between −5 T and 5 T. Amperometric measurements were carried out using an Autolab potentiostat, Model PGSTAT302N (Eco Chemie B.V.,). All the electrochemical measurements were carried out in a three-electrode thermostated cell at 25 °C with a platinum disk electrode as the working electrode (with a surface area of 0.0314 cm^2), a Pt counter electrode, and an Ag/AgCl (3 M KCl) electrode as a reference. The cell was protected from external electrical fields by a Faraday cage. Steady-state amperometric measurements were made as follows: the electrode was immersed in the aqueous solution and subjected to a voltage of +0.6 V vs. SCE. When the recorded signal attained a stable value, a known volume of a standard glucose solution was added with constant stirring. Subsequently, the signal variation corresponding to the oxidation of the enzymatically produced H_2O_2 was recorded. Prior to do any electrochemical measurements, the platinum electrodes were washed ultrasonically with hexane, acetone, isopropanol and distilled water. Then, they were heated at 60 °C for 30 s within a solution comprising a 1:1:5 volume ratio of aqueous ammonia (0.1 M), hydrogen peroxide (20%) and distilled water. Then, the electrode surfaces were polished with alumina slurry and any residual abrasive particles were ultrasonically removed. After that, 1 mg of particles were weighed and placed on the surface of the platinum electrode. Subsequently, the particles were covered and flattened around the electrode surface using a dialysis membrane MW 10 000. The resulting electrode was washed with phosphate buffer and overoxidized at +0.6 V until the background current decreased to a constant level.

2.3. Synthesis of silica magnetic nanoparticles covered with glucose oxidase

The synthesis of this material was carried out in several steps that are summarized in Scheme 1.

2.3.1. Step 1, synthesis of magnetic nanoparticles

Magnetic nanoparticles with diameters around 10 nm were synthesized using the Massart's coprecipitation method [15]. Briefly, a mixture of 8.6496 g of $FeCl_3{\cdot}6H_2O$ and 3.1213 g of $FeCl_2{\cdot}4H_2O$ were dispersed in 25 mL MiliQ-grade water and sonicated for 1 h. This mixture was poured into 250 mL of a solution of NaOH 1.5 M, which was thermostatized at 50 °C. The mixture was left to react for 30 min, under N_2 atmosphere and mechanical stirring. The sudden change in the pH affects the iron ion solution leading to the formation of iron oxide nanocrystals. Over this mixture, 10 g of stearic acid were added provoking the formation of a black precipitate formed by magnetic nanoparticles capped with stearic acid. These magnetic nanoparticles were separated by magnetic decantation and then they were washed with distilled water several times. The final product was dried and re-dispersed in chloroform at a concentration of 5 mg/mL.

2.3.2. Step 2, synthesis of the magnetic nanoparticles coated with silica

350 μL of the previously synthesized magnetic nanoparticles were mixed with 270 mg of polyoxyethylene(20) sorbitan monooleate. This solution was vigorously stirred with 4 mL of Milli-Q water during 45 min. With the aim of getting rid of the excess of surfactant, this mixture was centrifuged at 2500 rpm during 45 min. The supernatant was discarded, while the precipitate was collected and resuspended in 14 mL of water. This mixture was homogeneously dispersed in a solution of ethanol (40 mL) which contained 2.5 mL of concentrated ammonia aqueous solution (30%). After that, 4 mL ethanol containing 300 μL of TEOS was slowly added (0.07 mL/min) under mechanical stirring at room

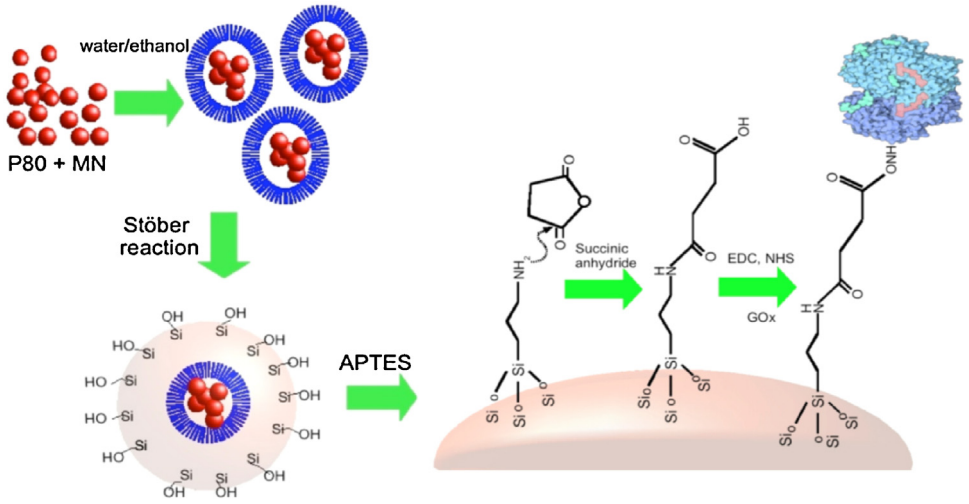

Scheme 1. Synthetic route used to prepare silica magnetic bioreactors.

temperature. This synthesis was named as S1. In other syntheses, the volume of ethanol used to disperse the magnetic clusters was increased from 40 mL to 50 mL (synthesis S2), and 70 mL (synthesis S3). That allowed to study the influence of the magnetic clusters concentration during the reaction. The products of these reactions were magnetically decanted and washed several times, collected with 20 mL of ethanol and stored for further reactions. The final particles concentration was ca. 5 mg/mL.

2.3.3. Step 3, surface functionalization and enzyme immobilization

With the aim of preparing the magnetic bioreactors, GOx was covalently anchored to the surface of the magnetic silica particles using APTES as linker. The APTES attachment was performed via chemical surface modification. The process was carried out by addition of 100 μL (0.45 mmol) of APTES to 5 mL of the as-prepared silica magnetic nanoparticles. This mixture was left to react overnight. After that, the particles were cleaned five times by centrifugation. This process yields an amine-terminated alkyl monolayer on the surface of silica magnetic nanoparticles. With the aim of inserting a carboxyl group where the enzyme will be attached via amide bond, the amino-modified nanoparticles were redispersed in 5 mL of anhydrous THF that contained 600 μL (0.5 mmol) of triethylamine and 430 mg (0.4 mmol) of succinic anhydride. This mixture was refluxed for 3 h under vigorous stirring (700 rpm). The amine terminal group reacts with the succinic anhydride, yielding a terminal carboxyl group. Later, the particles were cleaned five times by centrifugation and re-dispersed in 3 mL of phosphate buffer (50 mM, pH 7) which contained 10 μL (0.06 mmol) of N-ethyl-N8-dimethylaminopropyl-carbodiimide (EDC) and 20 mg (0.17 mmol) of N-hydroxysuccinimide (NHS). Both compounds (EDC and NHS) produce the carboxylic group activation required to link the enzymes. This mixture was left to react for 30 min at room temperature. After that, the samples were centrifuged at 3000 rpm for 10 min, collected and poured on 2 mL of a glucose oxidase (GOx) solution (25 mg/mL) under stirring for 2 h. Finally, the particles were cleaned five times by centrifugation and stored at 4 °C.

2.4. Protocol for determining the presence of primary amines

The amino-groups on the nanoparticle's surface were detected by an indirect fluorescent method. Briefly, 1 mL of an anhydrous dimethylformamide solution containing 6-[fluorescein-5(6)-carboxamido]hexanoic acid N-hydroxysuccinimide ester (0.02 M) was added drop wise to a 5 mL buffer solution at pH 9 containing 10 mg of γ-Fe_2O_3@SiO_2@APTES nanoparticles. This mixture was left to react for 1 h at room temperature. Then, the particles were centrifuged for at least three times at 2500 rpm. The resulting particles were redispersed with 5 mL of distilled water, obtaining a particle dispersion, which was ready for photoluminescence analysis.

3. Results

3.1. Synthesis and characterization of the magnetic nanoparticles

The Massart's coprecipitation method has been widely used to produce magnetic nanoparticles in high yield and with a high crystallinity and monodispersity. [22] In this work, we used a previously reported method [23] that permitted us to obtain iron oxide magnetic nanoparticles with a mean diameter close to 7 nm, as shown in Fig. 1. A variation of the synthetic conditions was the addition of stearic acid that provoked the precipitation of the nanoparticles due to the increment of their hydrophobicity.

Fig. 1A shows a representative TEM image of the synthesized magnetic nanoparticles. From the TEM image one can observe that the size of the nanoparticles obtained by coprecipitation was around 6.6 ± 1.7 nm (Fig. 1B). One of the most important characteristics of iron oxide nanoparticles is their magnetic moment which eventually determines their potential applications. The magnetic properties were studied by using a SQUID and the results are shown in Fig. 1C. The absence of hysteresis, which at low field is indicative of superparamagnetic behavior, suggests that each nanoparticle has only one magnetic domain. It is worth to note that the nanoparticle's magnetic moment do not fully saturate at high field as it is indicated by the absence of a clear plateau. This behavior is attributed to surface phenomena associated with the small size of the nanoparticles and their high specific surface. The crystalline structure of the magnetic nanoparticles was studied by X-ray diffraction. The diffraction pattern of these nanoparticles is presented in Fig. 2. The *d*-spacing of the reflections was calculated using the Bragg equation:

$$n \cdot \lambda = 2d \cdot \sin(\theta)$$

where λ = 1.541 Å is the X-ray wavelength and θ is the scattering angle. All detected diffraction peaks (see Table 1) are attributed to cubic γ-Fe_2O_3 phase (maghemite) or cubic Fe_3O_4 (magnetite). The Rietveld analysis showed that the γ-Fe_2O_3 phase represents

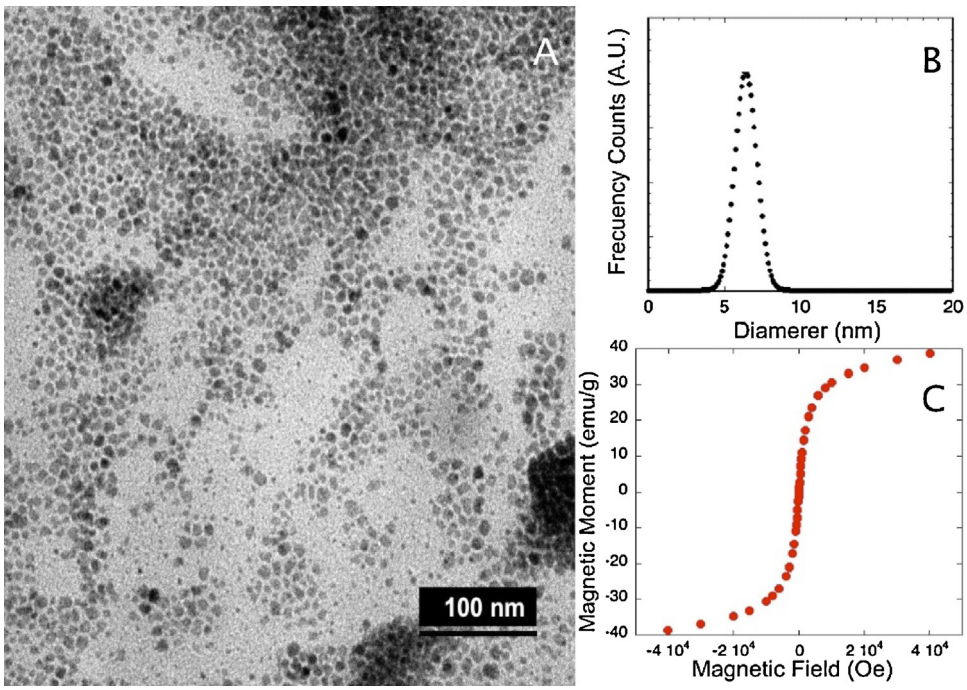

Fig. 1. (A) TEM micrograph of γ-Fe_2O_3 magnetic nanoparticles capped with stearic acid synthesized at 60 °C. (B) Size distribution of the nanoparticles measured by DLS. (C) Magnetization measurements of the nanoparticles.

Table 1
Position, *d*-spacing and Miller's indices of the reflections.

2θ (°)	30.34	35.65	43.54	53.82	57.54	63.02
d (Å)	2.944	2.517	2.078	1.702	1.601	1.474
h l k	(2 2 0)	(3 1 1)	(4 0 0)	(4 2 2)	(5 1 1)	(4 0 4)

93% of the crystalline contribution being the cubic Fe_3O_4 phase 7%. Furthermore, the calculated lattice parameter was found equal to 8.336 ± 0.004 Å, which is far closer to the lattice parameter of maghemite (8.351 Å) than that of magnetite (8.396 Å). These results indicate that the main crystalline phase of the synthesized nanoparticles could be identified as the cubic γ-Fe_2O_3 phase.

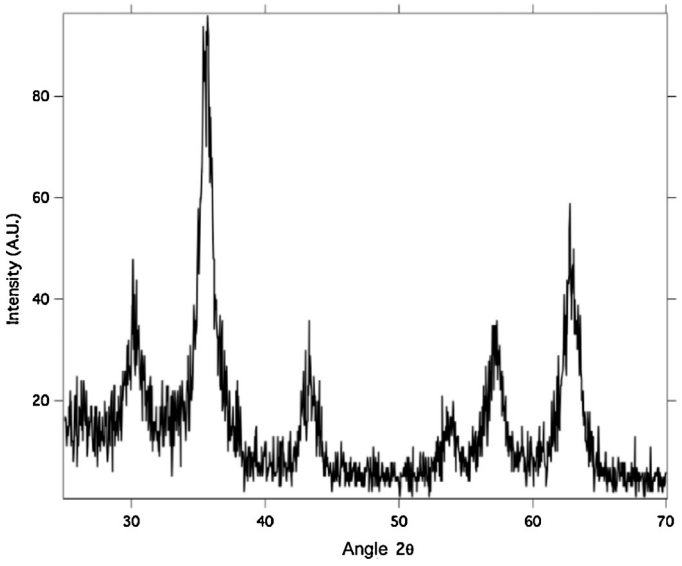

Fig. 2. X-ray diffraction pattern of the γ-Fe_2O_3 magnetic nanoparticles.

3.2. Synthesis of γ-Fe_2O_3@SiO_2 magnetic nanoparticles

The key point to obtain a magnetic core is the formation of magnetic clusters, which have to be stable in the ethanolic media in which the reaction takes place. This factor is crucial since the bare magnetic nanoparticles are unstable in ethanol. This problem can be circumvented by the convenient surface functionalization of the magnetic nanoparticles. For this reason, γ-Fe_2O_3 nanoparticles were covered with an aliphatic acid layer that provides hydrophobicity to the nanocrystals. Prior to their dispersion in the reaction media, the hydrophobic nanoparticles were mixed with a non-ionic surfactant (polysorbate 80), which interacts with the hydrophobic layer of the γ-Fe_2O_3 nanoparticles, stabilizing them. Thus, when the particles are dispersed in ethanol, they form magnetic clusters with a hydrodynamic diameter of 68 nm, with high colloidal stability, which can act as seeding points for the silica deposition (Fig. 3A). When the silica precursor (TEOS) is added to the magnetic cluster dispersion, the deposition of silica begins, yielding γ-Fe_2O_3@SiO_2 core@shell nanoparticles with a hydrodynamic diameter of 230 nm in case of synthesis S3 (see Fig. 3B). This result would indicate that effectively after incorporating TEOS in the reaction media the particles grow by the silica deposition.

Transmission electron microscopy was used to study the architecture adopted by the γ-Fe_2O_3@SiO_2 nanoparticles, see Fig. 4. In Fig. 4A we can observe that the silica deposition resulted in particles with magnetic cluster-cores. A detailed image of these samples revealed that the particles were formed by the agglutination of several nanoparticles of silica. This result was attributed to the high concentration of magnetic clusters

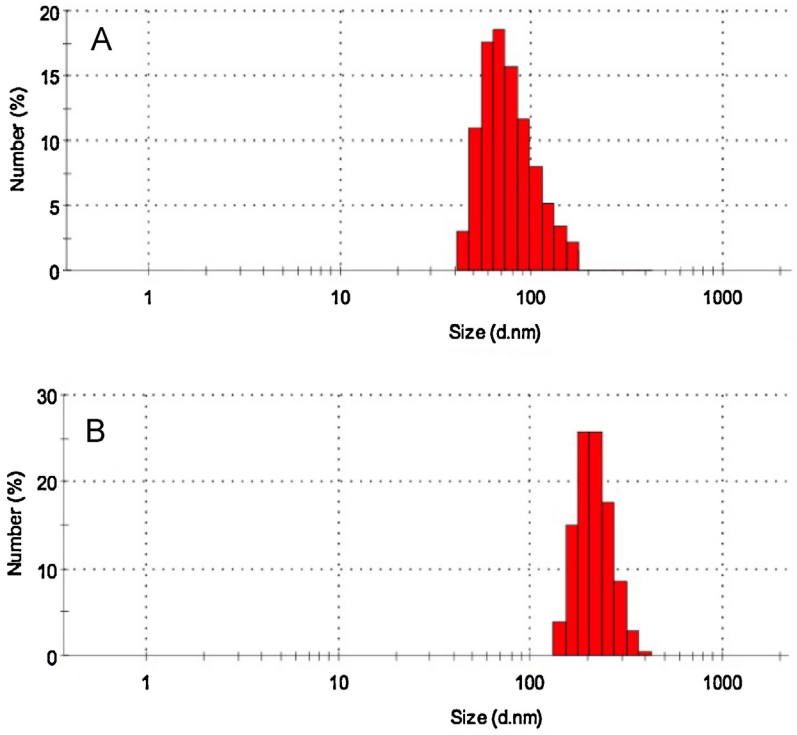

Fig. 3. Size distribution of (A) magnetic clusters in ethanol prior to the silica deposition, and (B) γ-Fe_2O_3@SiO_2 particles obtained after the silica deposition, reaction S3.

during the silica deposition. With the aim of reducing the size of the final γ-Fe_2O_3@SiO_2 nanoparticles, we performed the same reaction but decreasing the cluster concentration by increasing the volume of ethanol. Thus, when the amount of ethanol was increased up to 70 mL (synthesis S3) the size of the γ-Fe_2O_3@SiO_2 nanoparticles was reduced to 230 nm. Under this reaction conditions, the synthesis produced almost spherical particles and no signs of fused particles were observed. In consequence, these synthetic conditions were selected for the following experiments.

EDX microanalysis was performed in the previous sample to provide qualitative and quantitative determinations of the elemental composition. The microanalysis revealed the predominance of iron, with a K_α peak at 6400 eV and a K_β peak at 7059 eV and silicon with a K_α peak at 1740 eV (Fig. 5). From this spectrum, it was possible to estimate that the iron/silicon weight ratio in the sample was 1.1. Using this result and the molecular formula of the particles (γ-Fe_2O_3@SiO_2), we were able to infer the weight percentage of γ-Fe_2O_3 and SiO_2 in the particles, being 40% and 60%, respectively.

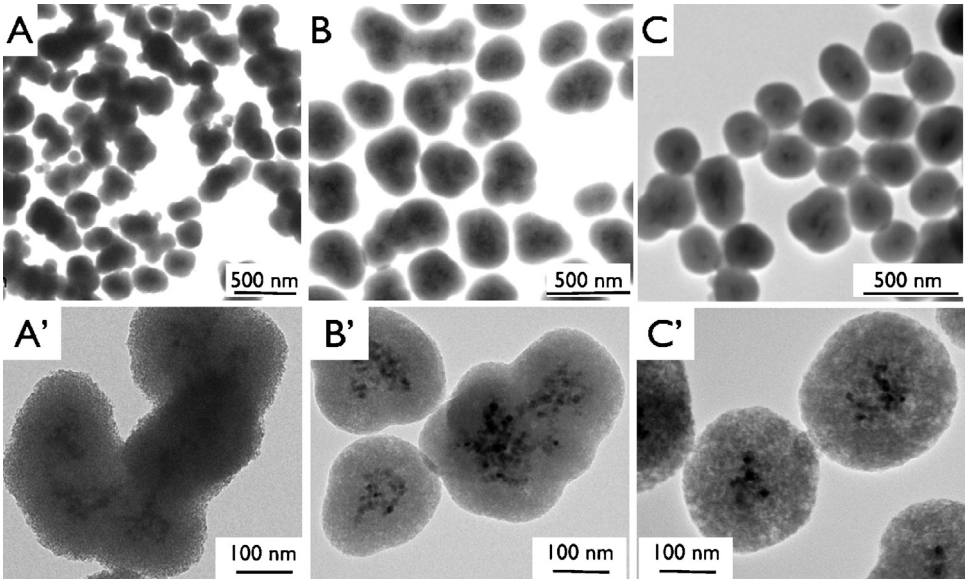

Fig. 4. The upper panel shows TEM micrographs of γ-Fe_2O_3@SiO_2 particles obtained after using different synthetic conditions. (A) γ-Fe_2O_3@SiO_2 produced in the synthesis S1, (B) γ-Fe_2O_3@SiO_2 produced in the synthesis S2 and (C) γ-Fe_2O_3@SiO_2 produced in the synthesis S3. The lower panel shows a detailed image of each synthesis.

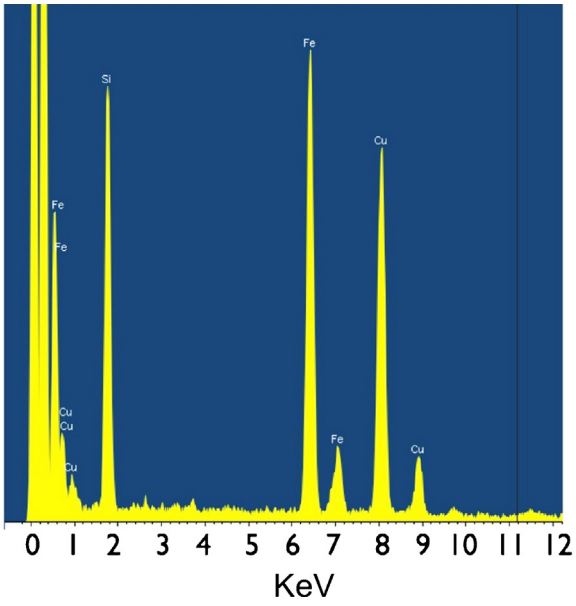

Fig. 5. Elemental EDX microanalysis of γ-Fe_2O_3@SiO_2 particles.

3.3. Immobilization of GOx on the surface of the γ-Fe_2O_3@SiO_2 magnetic nanoparticles

With the aim of making the surface suitable for the immobilization of enzymes or other biomolecules, γ-Fe_2O_3@SiO_2 particles were treated with APTES. The reaction between APTES and the γ-Fe_2O_3@SiO_2 yielded nanoparticles containing primary amines on the surface. After this reaction, the γ-Fe_2O_3@SiO_2-NH_2 particles were submitted to react with succinic anhydride in order to obtain carboxylic groups on the surface. To check the viability of these reactions, FTIR analyses were performed over γ-Fe_2O_3@SiO_2, γ-Fe_2O_3@SiO_2-NH_2 and γ-Fe_2O_3@SiO_2-COOH particles, respectively.

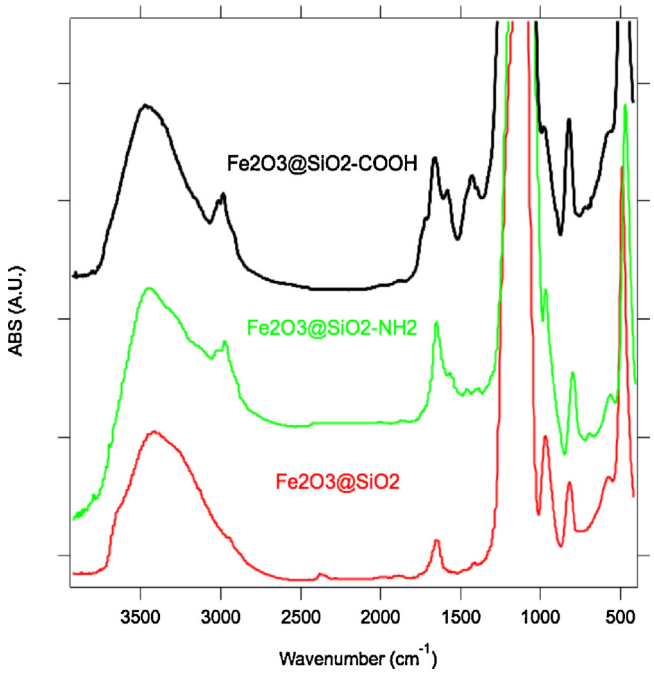

Fig. 6. FTIR spectra of (a) γ-Fe_2O_3@SiO_2 (red line), (b) γ-Fe_2O_3@SiO_2-NH2 (green line), and (c) γ-Fe_2O_3@SiO_2-COOH. (For interpretation of the references to color in this figure legend, the reader is referred to the web version of the article.)

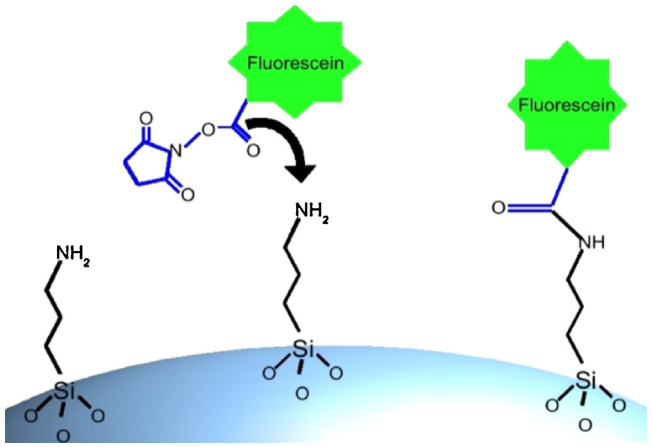

Scheme 2. synthetic route for labeling primary amines with fluorescein.

Fig. 6 shows the FTIR spectrum of the γ-Fe_2O_3@SiO_2. This spectrum showed the characteristic absorption peaks of silica located at 1100 cm^{-1}, 935 cm^{-1} and 750 cm^{-1}, which were attributed to the asymmetric stretching of the Si—O—Si, asymmetric stretching of Si—OH and the symmetric stretching of the Si—O—Si, respectively. The spectrum of the γ-Fe_2O_3@SiO_2-NH_2 particles showed new absorption bands at 2700–2900 cm^{-1}, which are characteristic of the CH_2 from APTES's residue. In addition, an increment of the peak intensity at 1630 cm^{-1} was observed. This peak could be attributed to the N—H bend of primary amines. Although the FTIR spectra revealed substantial changes in the absorption bands, in order to confirm that a layer with primary amines was introduced on the surface of the nanoparticles, we used an indirect method that specifically labels primary amines and turns them into fluorescent molecules [24]. This experiment involves using 6-[fluorescein-5(6)-carboxamido]hexanoic acid N-hydroxysuccinimide ester that binds covalently to primary amines. Scheme 2 shows the reaction that labels the primary amines with fluorescein.

Fig. 7 shows the fluorescent emission of the γ-Fe_2O_3@SiO_2-NH_2 particles (red line) after being labeled. These particles showed an intense emission peak at 520 nm, which corresponds with the emission value of the fluorescein.

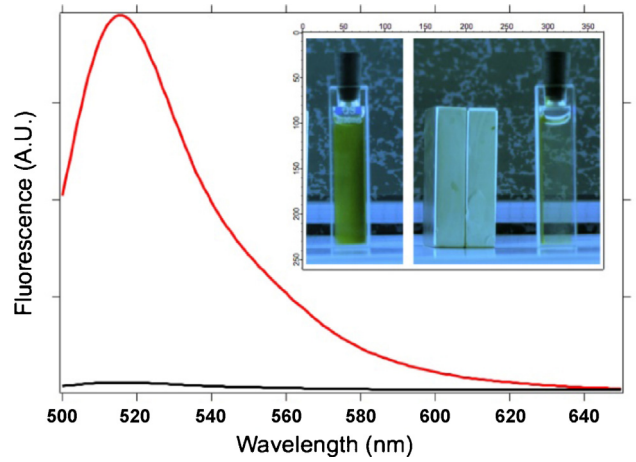

Fig. 7. Emission spectrum of (a) γ-Fe_2O_3@SiO_2-NH_2 particles labeled with fluorescein (red line) and (b) γ-Fe_2O_3@SiO_2 used as control experiment (black line). The inset shows the behavior of the γ-Fe_2O_3@SiO_2-NH_2 labeled with fluorescein under UV illumination in the absence and in the presence of a magnetic field. The excitation wavelength was 300 nm, $B = 0.4$ T. (For interpretation of the references to color in this figure legend, the reader is referred to the web version of the article.)

In order to prove that the emission peak was due to the presence of covalently attached fluorescein, we repeated the same reaction but using γ-Fe_2O_3@SiO_2 instead of γ-Fe_2O_3@SiO_2-NH_2. This reaction resulted in silica particles with a faint fluorescent emission at 520 nm, which was attributed to the physical adsorption of some molecules of fluorescein (Fig. 7, black line). In addition, the presence of an external magnetic field close to fluorescent dispersion provoked the migration of the particles toward the cuvette wall (see inset of Fig. 7), demonstrating the magnetic responsiveness of the resulting material. In summary, this experiment clearly indicates that the introduction of primary amines was successfully achieved.

Subsequently, the γ-Fe_2O_3@SiO_2-NH_2 particles were submitted to react with succinic anhydride to introduce carboxylic groups on the surface of the nanoparticles, which were used as anchoring points for the enzyme immobilization. The FTIR spectrum of γ-Fe_2O_3@SiO_2-COOH nanoparticles showed the existence of new bands at 1558 cm^{-1} and 1403 cm^{-1} which correspond to the asymmetric and symmetric stretching vibration of the COO^- groups, respectively. In addition, new peaks attributed to the amide I band and amide II band located at 1689 cm^{-1} and 1635 cm^{-1} were also seen. These results could indicate that COO^- groups have been incorporated on the surface of the nanoparticles. For the immobilization of glucose oxidase (GOx) on the surface, the carboxylic groups of the nanoparticles were activated with EDC and NHS. Subsequently, they were exhaustively rinsed with phosphate buffer 50 mM at pH 7. Then, the particles were dropped onto a GOx solution under mechanical stirring and left to react for 2 h. This step led to the covalent immobilization of GOx on the surface of the γ-Fe_2O_3@SiO_2-COOH nanoparticles. With the aim of establishing the amount of enzyme that these particles could adsorb, we repeated the same experiment, but without using the coupling reagents (EDC and NHS). The enzymatic activity of these samples was measured and established as negligible in comparison with the sample in which the enzyme was covalently attached.

3.4. Study of the enzymatic activity of the γ-Fe_2O_3@SiO_2-GOx particles

To prove the efficiency of the immobilization process as well as the enzymatic activity of the enzyme, we used the magnetic silica particles with GOx as a component of an amperometric glucose biosensor. The mechanism for GOx catalyzed reaction is a ping-pong type and can be outlined as follows:

$$E + G \underset{k_{-1}}{\overset{K_1}{\rightleftharpoons}} E - G \xrightarrow{K_2} E^{\bullet} + \text{gluconatolactone}$$

$$E^{\bullet} + O_2 + H_2O \underset{k^a_{-1}}{\overset{K^a_1}{\rightleftharpoons}} E^{\bullet} - O_2 \xrightarrow{K^a_2} E + H_2O_2$$

where E is the enzyme, G the substrate (glucose) and $E-G$ and $E^{\bullet}-O_2$ are the addition complexes. The oxygen consumption rate is represented by the Michaelis–Menten equation with the apparent K^O_m.

$$K^{app} = \frac{K^O_m}{1 + K^G_m/G}$$

being

$$K^O_m = \frac{K^a_{-1} + K^a_2}{K^a_1}$$

$$K^G_m = \frac{K_{-1} + K_2}{K_1}$$

This reaction was monitored by amperometry, since the hydrogen peroxide formed during the enzyme-catalyzed reaction can be oxidized on the surface of a platinum electrode at +0.6 V vs. Ag/AgCl, generating a current response, which is measured. In this kind of system, the steady-state current, i_k, for an amperometric enzyme electrode under kinetic control is given by the equation:

$$i_k = \frac{i_{max} \cdot [S]}{K^{app} + [S]}$$

where i_{max} is the maximum current response which is proportional to the concentration of GOx, [S], the substrate concentration and K^{app} is the apparent Michaelis–Menten constant. i_{max} is related with the amount of enzyme immobilized on the silica particles by the following equation:

$$i_{max} = \frac{nFAd}{2} K_c [E_0]$$

where n is the number of electrons that take part of the redox reaction at the electrode surface, F is the Faraday constant, A is the electrode area, d is the diffusion layer thickness, k_c is the catalytic constant and $[E_0]$ is the concentration of enzyme placed on the electrode.

The current responses of glucose biosensors constituted by 1 mg of γ-Fe_2O_3@SiO_2-GOx particles and 1 mg of free GOx are shown in Fig. 8a. After the immobilization of the enzyme, the particles were able to catalyze the oxidation of the glucose. In this reaction, GOx produced hydrogen peroxide, which was transformed into a current density response that was proportional to the glucose consumed in the process. This response followed a Michaelis–Menten kinetics with K^{app} = 10 mM and $i_{max} = 26 \times 10^{-6}$ A/cm^2. This result was compared with the response produced by 1 mg of free GOx placed on the electrode, showing that 1 mg of free GOx produced a signal six-fold greater than the GOx immobilized on the surface of the particles. With this result, we could estimate a loading capacity for the magnetic silica particles close to 20% in weight (w/w), assuming that the catalytic constant (k_{cat}) is similar for the immobilized enzyme and for the free enzyme. Furthermore, we observed an increment of the K^{app} to 10 mM for the immobilized GOx, which would suggest a loss of substrate affinity as consequence of the enzyme immobilization. This effect could be related with the fact that some enzymes oriented their catalytic center toward the surface of the particle, reducing their possibility of interacting with the substrates.

In addition, the linearity of the biosensor constituted by γ-Fe_2O_3@SiO_2-GOx particles was maintained in the range 0.1–10 mM glucose as is illustrated in Fig. 8b. The response of this biosensor follows the equation $y = 1.1 \times 10^{-8} + 1.5x$ (with $r = 0.999$), being y the current density expressed in A/cm^2 and x the substrate concentration in mM. A detection limit of 0.03 mM was estimated with a signal-to-noise ratio equal to 3. The Fig. 8c depicts a schematic view of the biosensor designed using the γ-Fe_2O_3@SiO_2-GOx nanoparticles with immobilized GOx as biological component.

3.5. Stability and reusability

In order to study the stability of the immobilized enzyme, different measurements were performed using the biosensors prepared with γ-Fe_2O_3@SiO_2-GOx particles and with free GOx. The results showed that the stability of the enzyme was enhanced when it was immobilized, in such a way that it retained the 80% of its initial activity after 14 days. By contrast, the enzymatic activity of the free enzyme dropped down to 40% in the same period (see Fig. 9A). These experiments demonstrate that the covalent immobilization of the enzyme slightly improves its stability. Furthermore, if we compare the stability of the biosensors prepared by covalent attachment of the enzyme with the stability of those prepared by using electrostatic interactions [31] it is observed that the covalent immobilization could provide better enzymatic stability. However,

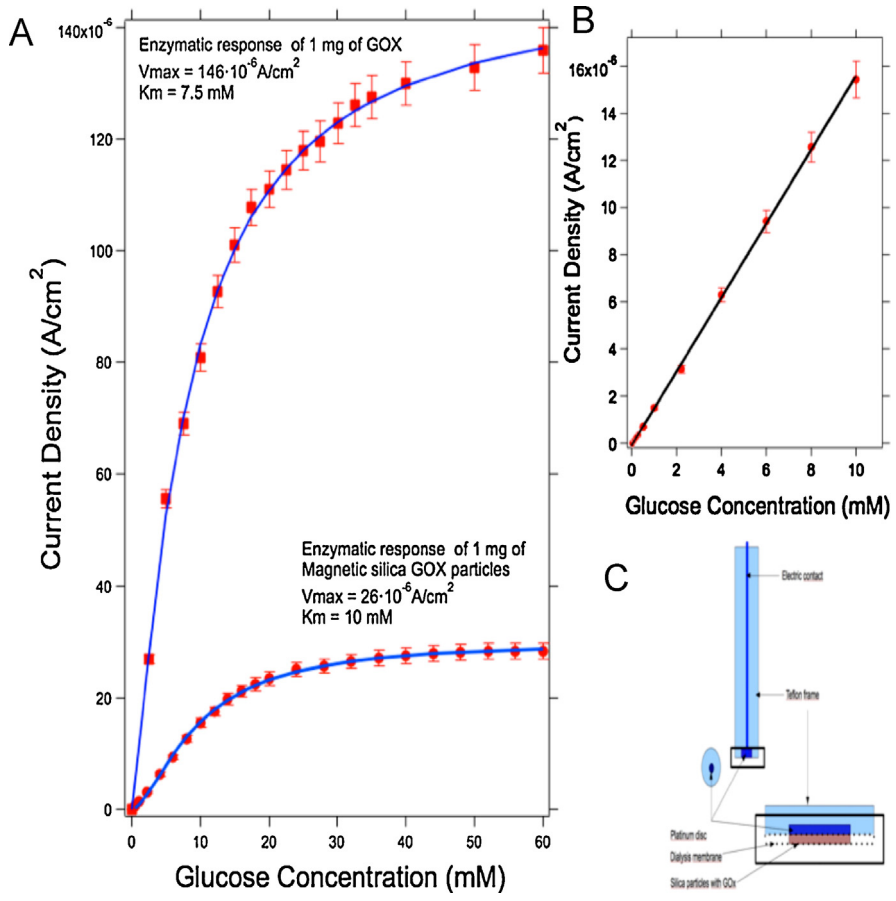

Fig. 8. (a) Current response of 1 mg of free GOx and 1 mg of magnetic silica GOx particles placed on the surface of the working electrode, (b) linear range of the biosensor formed by 1 mg of γ-Fe_2O_3@SiO_2-GOx particles and (c) schematic representation of the biosensor setup. Each point represents the mean value ± SD of the current response from three replicate measurements.

this result is not conclusive since it was performed with different enzymes, GOx and acetyl choline (AChE), respectively.

With the aim of determining the reusability of the γ-Fe_2O_3@SiO_2-GOx nanoparticles, 10 mg were poured into 10 mL of phosphate buffer at pH 7 containing 100 mM of glucose. After 30 min in this solution, hydrogen peroxide was detected and related with the enzymatic activity of the γ-Fe_2O_3@SiO_2-GOx nanoparticles. Afterwards, the particles were magnetically recovered, the

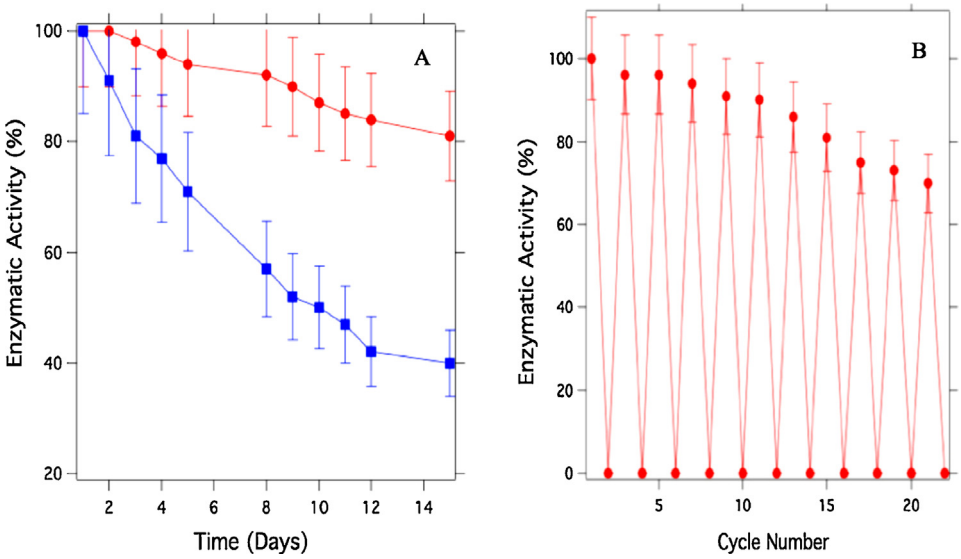

Fig. 9. Enzymatic activity as a function of the time for (a) γ-Fe_2O_3@SiO_2-GOx particles (red line) and (b) free GOx (blue line). (b) Reusability test of the γ-Fe_2O_3@SiO_2-GOx particles. Each point represents the mean value ± SD of the current response from three replicate measurements. (For interpretation of the references to color in this figure legend, the reader is referred to the web version of the article.)

supernatant discarded, and finally the particles were washed with phosphate buffer and re-dispersed in the reaction media. This process was repeated several times and the enzymatic response of the γ-Fe_2O_3@SiO_2-GOx nanoparticles was plotted as a function of the cycle number (see Fig. 9B). The results showed that the system maintained the enzymatic activity (above 90% of the initial value) during at least 5 cycles. After that, the activity dropped down, which could be due to the sum of two different effects; the loss of particles during the washing processes and the inherent enzyme denaturalization that occurs along the experiments.

4. Conclusion

In this work we present a synthetic method to produce magnetic-responsive bioreactors based on functionalized silica particles with iron oxide cores. This method permitted to produce spherical γ-Fe_2O_3@SiO_2 with 200 nm of diameter and an γ-Fe_2O_3 content of 40% in weigh. A surface-chemistry modification was performed to allow the covalent immobilization of enzymes (GOx), which provided catalytic activity to the system. This property was analyzed by employing the magnetic silica particles with GOx as components of an amperometric biosensor. The analysis of the enzymatic response permitted to determine that the amount of GOx immobilized on the surface was around 20% (w/w). In addition it was possible to observe an increment of the K^{app} for the immobilized enzymes that was attributed to the loss of enzymatic affinity for the substrate. This effect was related with the steric restrictions that the immobilization process induced on the catalytic center of the enzymes. The stability study confirmed that the immobilization process enhanced significantly the enzymatic stability and allowed its reuse.

Acknowledgments

The authors acknowledge financial support from the Spanish Science and Innovation Ministry (Grant MAT2010-15349) and from COST Action CM1101. Paulino Alonso-Cristobal acknowledges the Spanish Research Ministry for an FPU fellowship to perform this work. Marco Laurenti acknowledges the Comunidad of Madrid for a fellowship to perform this work. We want also to thank Agustin Fernandez from UCM-microscopy CAI for his help with TEM micrograph and the fruitful discussion.

References

[1] I. Chibata, Immobilized Enzymes. Research and Development, Kodansha, Tokyo, 1978.
[2] L. Goldstein, E. Katchalski-Katzir, in: L.B. Wingard Jr., E. Katchalski-Katzir, L. Goldstein (Eds.), Immobilied Enzyme Principles. Series Applied Biochemistry and Bioengineering, vol. 1, Academic Press, New York, 1976, pp. 1–22.
[3] J. Rubio-Retama, E. López-Cabarcos, B. López-Ruiz, High stability amperometric biosensor based on enzyme entrapment in microgels, Talanta 68 (1) (2005) 99–107.
[4] S. Solis, J. Paniagua, J.C. Martinez, M. Asomoza, Immobilization of papain on mesoporous silica: pH effect, J. Sol–Gel Sci. Technol. 37 (2) (2006) 125–127.
[5] B. Zhao, B. Shi, R. Ma, Immobilization of papain on the mesoporous molecular sieve MCM-48, Eng. Life Sci. 5 (5) (2005) 436–441.
[6] A. Bhardwaj, J. Lee, K. Glauner, S. Ganapathy, D. Bhattacharya, D.A. Butterfield, Biofunctional membranes: an EPR study of active site structure and stability of papain non-covalently immobilized on the surface of modified poly (ether) sulfone membranes through the avidin–biotin linkage, J. Membr. Sci. 119 (2) (1996) 241–252.
[7] H. Eckstein, H.J. Renner, H. Brun, Immobilization of papain on epoxy-polymers for papain-catalyzed peptide synthesis, Biomed. Biochim. Acta 50 (10–11) (1991) S114–S117.
[8] R.Y.-Y. Chiou, L.R. Beuchat, Immobilization of papain on an anion exchange resin by physical adsorption followed by cross linking with glutaraldehyde, J. Food Biochem. 11 (2) (1987) 163–176.
[9] P. Pfromm, K. Würges, Lyophilizate of an enzyme and fumed silica for enzymatic catalysis in non-aqueous solvents, PCT Int. Appl. (2006) 32.
[10] R.A. Gross, B. Chen, M.E. Miller, J.C. Bohling, Abstracts of papers, in: 230th ACS National Meeting, Washington, DC, August 28–September 1, 2005.
[11] S. Hong, P.R. Leroueil, E.K. Janus, J.L. Peters, M.M. Kober, M.T. Islam, B.G. Orr, J.R. Baker Jr., H. Banaszak, M. Mark, Interaction of polycationic polymers with supported lipid bilayers and cells: nanoscale hole formation and enhanced membrane permeability, Bioconjugate Chem. 17 (3) (2006) 728–734.
[12] Q.A. Pankhurst, J. Connolly, S.K. Jones, J. Dobson, Applications of magnetic nanoparticles in biomedicine, J. Phys. D: Appl. Phys. 36 (2003) R167–R181.
[13] T. Shao-Long, L. Hyeon-Cheol, B. Youn-Sang, K. Min-Bae, L. Kangtaek, L. Chang-Ha, Monodisperse Fe_3O_4/Fe@SiO_2 core/shell nanoparticles with enhanced magnetic property, Colloids Surf. A: Physicochem. Eng. Aspects 293 (2007) 278–285.
[14] S. Laurent, D. Forge, M. Port, A. Roch, C. Robic, L.V. Elst, R.N. Muller, Magnetic iron oxide nanoparticles: synthesis, stabilization, vectorization, physicochemical characterizations, and biological applications, Chem. Rev. 108 (2008) 2064–2070.
[15] Yu. Han, J. Jiang, S.S. Lee, J.Y. Ying, Reverse microemulsion-mediated synthesis of silica-coated gold and silver nanoparticles, Langmuir 24 (11) (2008) 5842–5850.
[16] Yu. Lu, Y. Yin, B.T. Mayers, Y. Xia, Modifying the surface properties of superparamagnetic iron oxide nanoparticles through a sol–gel approach, Nano Lett. 2 (3) (2002) 186–193.
[17] W. Stöber, A. Fink, E. Bohn, Controlled growth of monodisperse silica spheres in the micron size range, J. Colloid Interface Sci. 26 (1968) 62–69.
[18] M. Ohmori, E. Matijević, Preparation and properties of uniform coated colloidal particles VII. Silica on hematite, J. Colloid Interface Sci. 150 (1992) 594.
[19] A.P. Philipse, M.P.B.V. Bruggen, C. Pathmamanoharan, Magnetic silica dispersions: preparation and stability of surface-modified silica particles with a magnetic core, Langmuir 10 (1) (1994) 92–99.
[20] L.M. Liz-Marzán, M. Giersig, P. Mulvaney, Synthesis of nanosized gold-silica core–shell particles, Langmuir 12 (18) (1996) 4329–4330.
[21] C. Graf, D.L.J. Vossen, A. Imhof, A.V. Blaaderen, A general method to coat colloidal particles with silica, Langmuir 19 (17) (2003) 6693–6700.
[22] R. Massart, Preparation of aqueous magnetic liquids in alkaline and acidic media, IEEE Trans. Magn. 17 (1981) 1247.
[23] D. Serrano-Ruiz, S. Rangou, A. Avgeropoulos, N.E. Zafeiropoulos, E. López-Cabarcos, J. Rubio-Retama, Synthesis and chemical modification of magnetic nanoparticles covalently bound to polystyrene $SiCl_2$ poly(2 vinylpyridine), J. Polym. Sci. B: Polym. Phys. 48 (2010) 1668–1670.
[24] J. Díaz, I. Barasoain, A.A. Souto, F. Amat-Guerri, J.M. Andreu, Macromolecular accessibility of fluorescent taxoids bound at a paclitaxel binding site in the microtubule surface, J. Biol. Chem. 280 (5) (2005) 3928–3937.
[25] X. Luo, L. Zhang, Immobilization of penicillin G acylase in epoxy-activated magnetic cellulose microspheres for improvement of biocatalytic stability and activities, Biomacromolecules 11 (2010) 2896–2900.
[26] Y. Hih-Hao, A. Al-Saadi, S. Shih, L. Qiu, K.Y. Tam, S.C. Tsang, Immobilization of BSA on silica-coated magnetic iron oxide nanoparticle, J. Phys. Chem. C 113 (2) (2009) 537–543.
[27] A. Dyal, K. Loos, N. Noto, S.W. Chang, C. Spagnoli, V.P.M.S. Kurikka, A. Ulman, M. Cowman, R.A. Gross, Activity of *Candida rugosa* lipase immobilized on ε-Fe_2O_3 magnetic nanoparticles, J. Am. Chem. Soc. 125 (7) (2003) 1684–1690.
[28] Y. Hee-Man, W.P. Chan, W. Min-Ah, I.K. Moon, M.J. Yeong, G.P. Hyun, K. Jong-Duk, HER2/neu antibody conjugated poly(amino acid)-coated iron oxide nanoparticles for breast cancer MR imaging, Biomacromolecules 11 (11) (2010) 2866–2870.
[29] R.H. Aimee, K. Byeong-Su, T.A. Taton, Encapsulated magnetic nanoparticles as supports for proteins and recyclable biocatalysts, Bioconjugate Chem. 18 (1) (2007) 183–189.
[30] M. Kalantari, M. Kazemeini, F. Tabandeh, Y. Arpanaei, Lipase immobilisation on magnetic silica nanocomposite particles: effects of the silica structure on properties of the immobilised enzyme, J. Mater. Chem. 22 (2012) 8385–8390.
[31] Y.H. Won, H.S. Jang, S.M. Kim, E. Stach, M. Ganesana, S. Andreescu, L.A. Stanciu, Biomagnetic glasses: preparation, characterization and biosensor applications, Langmuir 26 (6) (2010) 4320–4330.